Two-particle two-hole configurations in ^{208}Bi and the ^{210}Bi$^m(p,t)^{208}$Bi reaction

K. A. Erb and W. D. Callender*
A. W. Wright Nuclear Structure Laboratory, Physics Department, Yale University, New Haven, Connecticut 06520

R. K. Sheline
The Florida State University, Tallahassee, Florida 32306

(Received 19 April 1979)

Levels in ^{208}Bi were studied using the ^{210}Bi$^m(p,t)^{208}$Bi reaction at 18.4 MeV. The target isomeric state employed in the reaction was the 9^-, 271 keV, 3×10^6 year second-excited state of ^{210}Bi. The measured angular distributions for the positive parity $(\pi h_{9/2},\nu^{-1})$ particle-hole multiplets were well described by distorted-waves calculations using the shell model wave functions of Kuo. However, the data for the negative parity $(\pi h_{9/2},\nu^{-1}i_{13/2})$ levels were poorly reproduced by these calculations, and evidence was found for the presence of two-particle two-hole admixtures in the 9^-, 10^-, and 11^- members of this multiplet. In addition, a number of previously unobserved levels were identified in ^{208}Bi, and several of these were populated in the reaction with considerably enhanced cross sections. The excitation energies and differential cross sections for the latter group of levels were found to be characteristic of two-particle two-hole states in ^{208}Bi consisting of $\pi h_{9/2},\nu g_{9/2}$ particles coupled to the 0_1^+ and 2_1^+ excitations of ^{206}Pb.

[NUCLEAR REACTIONS ^{210}Bi$^m(p,t)^{208}$Bi, $E=18.4$ MeV; measured $\sigma(\theta)$. ^{208}Bi deduced levels, J, π. Radioactive, enriched target. DWBA analysis, tested shell model wave functions.]

I. INTRODUCTION

The proton-particle neutron-hole multiplets observed[1-5] in ^{208}Bi have been a rich source of information concerning residual interactions and the effects of model space truncation in the nuclear shell model.[6-9] The predominantly one-particle one-hole nature of the low-lying states in this nucleus is well documented,[1,2,4] and has been accurately reproduced in several theoretical studies.[7-9] At higher excitation energies, where the influence of core excitations might become significant, little is known experimentally to either motivate or guide the theoretical study of these more complicated configurations.

In the present paper we exploit the properties of the ^{210}B$^m(p,t)^{208}$Bi reaction to search for core-excited structures in ^{208}Bi. The radioactive ^{210}Bi^m target ($\tau_{1/2}=3\times10^6$ yr) has several unusual advantages for this purpose, with its uniquely high spin ($J^\pi=9^-$) and essentially pure $(\pi h_{9/2},\nu g_{9/2})$ structure. The 9^- target spin leads to the population of high spin levels in ^{208}Bi which would be otherwise inaccessible to the (p,t) reaction, while the target structure enables the direct population of both one-particle one-hole and two-particle two-hole configurations. Both types of structure were observed in ^{208}Bi in the present study. For the former, distorted-waves calculations were compared with the measured yields to provide a test of the associated wave functions. For the latter, the relationships between measured ^{208}Pb$(p,t)^{206}$Pb and ^{210}Bi$^m(p,t)^{208}$Bi cross sections implied by the weak coupling model were examined to determine the extent to which these two-particle two-hole structures are based on simple core excitations.

II. EXPERIMENTAL PROCEDURES AND RESULTS

Differential cross sections for the ^{210}Bi$^m(p,t)^{208}$Bi reaction were measured in 7.5° steps, using 18.4 MeV protons from the Yale MP tandem Van de Graaff and the multiangle magnetic spectrograph.[10] The ^{210}Bi^m was deposited on a 2 mm×3 mm spot on a 60 μg/cm^2 carbon foil, which in turn was mounted on an aluminum frame. The ^{210}Bi^m target material was produced by exposing normal monoisotopic metallic ^{209}Bi to the neutron flux of the Savannah River Laboratory of the Atomic Energy Commission. After the 5 d ^{210}Bi ground state activity decayed away, the long lived ^{210}Bi^m was separated in a first pass at the Oak Ridge calutron, producing 2.5% ^{210}Bi^m in ^{209}Bi. The second isotope separation of 33 μg of ^{210}Bi^m in 1.39 mg of total Bi was carried out with the Florida State University isotope separator. This separation, which has been described elsewhere,[11] yielded an isotopic purity of >99% ^{210}Bi^m.

Elastic scattering yields of protons from the ^{210}Bi^m target were monitored throughout the experiment using a silicon surface barrier detector mounted in the scattering chamber. These yields

were compared at periodic intervals with proton elastic scattering from a ^{209}Bi target whose thickness was known accurately from previous measurements. In this way an effective, average thickness of 5.40 μg/cm^2 was determined for the ^{210}Bi^m target during the ^{210}Bi$^m(p,t)^{208}$Bi exposure.

Ilford K-5 emulsions, 50 μm in thickness, were used to record the tracks of the tritons at the focal plane of the magnet. To compensate for the thinness of the target, the plates were exposed for 84 000 μC of collected charge. The developed plates were scanned in $\frac{1}{2}$ mm steps. Absolute cross sections were determined using the effective target thickness, integrated beam charge, and the known properties of the magnetic spectrograph. These cross sections are accurate to within 25%. The energy resolution in the triton spectra varied from 10 to 15 keV, being typically 12 keV, FWHM.

A spectrum measured at 27.5° is plotted in terms of reaction Q value in Fig. 1. The excitation energies of levels observed in the present work are listed in Tables I and II. (For several of these excitation energies, no peaks are evident in the figure; however, the corresponding levels were observed in at least four other spectra, at widely spaced angles.) Although the experiment was sensitive to cross sections as small as 1 μb/sr, complete angular distributions could be extracted only for levels populated with cross sections in excess of 5 μb/sr. The angular distribution data are plotted in Figs. 2–5.

For purposes of comparison, the positions of the members of the one-particle one-hole multiplets are indicated at the top of Fig. 1. Most of these could be identified in at least several spectra, and, in addition, a number of previously unobserved states were identified in the present study.

III. DISTORTED WAVES CALCULATIONS

Distorted waves Born approximation (DWBA) calculations were carried out using the two-nucleon transfer version of the code DWUCK.[12] The optical model parameters for the proton channel were taken from the work of Perey,[13] and those for the triton channel from Flynn *et al.*[14] The parameters are listed in Table III. The predicted DWBA cross section (expressed in μb/sr) is given by Baer *et al.*[15] in terms of the DWUCK output as

$$\frac{d\sigma}{d\Omega}=\epsilon D_0^2\times 9.67\times 10^4 \sum_L (2L+1)^{-1}(d\sigma/d\Omega)^L_{\text{DWUCK}}.$$

We found it necessary to include all allowed L transfers ≤ 8 in the calculations. The constant, D_0^2, is commonly taken as an overall normalization factor, and has been determined empirically in studies involving somewhat lighter nuclei to be approximately 22.[15,16] In the present study a somewhat larger value, $D_0^2=27.5$, was required for a good overall fit to the data. The multiplicative factor, ϵ, should be equal to 1 if the reaction mechanism and nuclear wave functions are properly described.

The DWUCK form factor[15] for the two-nucleon transfer consists of the coherent superposition of two-neutron configurations,

$$F_{LS}(r)=\sum_{j_1 j_2} B(j_1 j_2; J) F_{LS}^{j_1 j_2}(r),$$

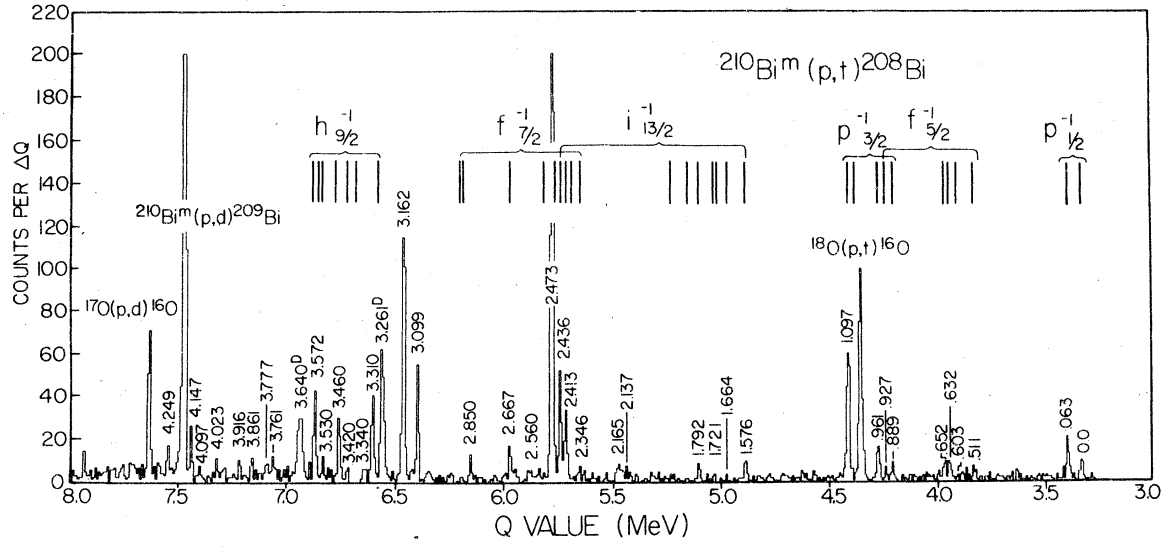

FIG. 1. Yields from the ^{210}Bi$^m(p,t)^{208}$Bi reaction measured at 27.5° and plotted as a function of reaction Q value. The excitation energies of the ($\pi h_{9/2}$, ν^{-1}) multiplet members are indicated at the top of the figure.

TABLE I. One-particle one-hole states observed in the present study.

Neutron-hole configuration	Excitation energy [a]	J^π	ϵ (pure configuration)	ϵ (Kuo wave functions)
$3p_{1/2}$	0.0	5^+	1.0	1.2
	0.063	4^+	1.0	1.5
$2f_{5/2}$	0.511	6^+	1.0	1.5
	0.603	4^+		
	0.632	$3^+, 5^+$ [b]	1.3	1.3
	0.652	7^+		
	0.927	2^+	1.0	1.0
$3p_{3/2}$	0.889	5^+	1.0	1.0
	0.961	4^+	1.9	1.0
	1.097	6^+	1.1	1.1
$1i_{13/2}$	1.576	10^-	4.0	4.0
	1.664	8^-		
	1.721	$6^-, 7^-$		
	1.792	9^-	(5.0)	(5.0)
	2.436	11^-	7.6	7.6
$2f_{7/2}$	2.346	7^+		
	2.667	8^+	1.0	1.0

[a] Excitation energies from Ref. 4.
[b] Unresolved in some spectra. The combined yields were analyzed.

TABLE II. Levels observed in addition to the one-particle one-hole states listed in Table I. The transition strengths listed in the last column represent observed fragments of the corresponding unfragmented core-excited strength, as discussed in the text.

$E \pm \Delta E$ (MeV ± keV)	L transfer	J^π	$N_f \frac{(2J_f+1)}{(2J_c+1)(2J_i+1)}$
2.137 ± 7			
2.165 ± 7			
2.413 ± 5	0	9^-	0.08
2.473 ± 5	0	9^-	0.82
2.560 ± 5			
2.850 ± 7			
3.099 ± 5	2	J^-	0.09
3.162 ± 5	2	J^-	0.26
3.261 [a] ± 10			
3.310 [a] ± 10	2	J^-	0.19
3.340 ± 7			
3.420 ± 10			
3.462 ± 5	2	J^-	0.08
3.530 ± 7	0	9^-	0.03
3.572 ± 5	2	J^-	0.12
3.640 [a] ± 7			
3.761 ± 7			
3.777 ± 10			
3.861 ± 5			
3.916 ± 10			
4.023 ± 10			
4.097 ± 10			
4.147 ± 5			
4.249 ± 5			

[a] Unresolved doublet.

where $B(j_1 j_2; J)$ is the spectroscopic amplitude defined by Yoshida,[17]

$$B(j_1 j_2; J) = (2J_i+1)^{-1/2} \langle \psi(N) J_i \| A^{\dagger J}_{j_1 j_2} \| \psi(N-2) J_f \rangle$$

in terms of the transfer operator,

$$A^{\dagger JM}_{j_1 j_2} = \sum_{m_1(m_2)} \langle j_1 m_1 j_2 m_2 | JM \rangle a^\dagger_{j_1 m_1} a^\dagger_{j_2 m_2}.$$

The wave functions describing the initial and final nuclear states must be specified before the spectroscopic amplitude can be calculated. The ^{210}Bi^m target state consists of an essentially pure pure[18,19] proton-neutron configuration,

$$|\psi(N) J_i\rangle = |\pi(j) \nu(j_1) J_i\rangle,$$

with $\pi(j) = \pi(1h_{9/2})$, $\nu(j_1) = \nu(2g_{9/2})$, and $J_i = 9$.

In the ^{208}Bi residual nucleus the configuration mixing of the one-particle one-hole multiplets at low excitation energies is predicted[7-9] to be slight, but of a magnitude which nonetheless can lead to significant effects in the two nucleon transfer cross sections. These small admixtures are therefore retained in the description of the proton-particle neutron-hole residual states:

$$|\psi(N-2) J_f\rangle = \sum_{p,h} a_{ph} |\pi(j) \nu^{-1}(j_2) J_f\rangle.$$

With these wave functions the spectroscopic amplitudes can be reduced to

TABLE III. Optical model parameters used in the DWBA calculations.

	V (MeV)	r (fm)	a (fm)	W (MeV)	$4W_D$ (MeV)	r_i (fm)	a_i (fm)	r_c (fm)
p [a]	54.5	1.25	0.650	0.0	71.2	1.25	0.470	1.25
t [b]	166.7	1.16	0.752	10.0	0.0	1.498	0.817	1.25
n	c	1.25	0.650					1.25

[a] From Ref. 13.
[b] From Ref. 14.
[c] Adjusted to give each orbit a binding energy of $-0.5(S_{2n}+E_x)$, where S_{2n} is the two-neutron separation energy and E_x is the excitation energy in the residual nucleus.

$$B(j_1 j_2; J) = (-1)^{j+j_2+J+J_i+1} \times[(2J+1)(2J_f+1)]^{1/2} a_{\rm ph} \begin{Bmatrix} J_f & j & j_2 \\ j_1 & J & J_i \end{Bmatrix}$$

$$= (-1)^{9/2+j_2+J} \times[(2J+1)(2J_f+1)]^{1/2} a_{\rm ph} \begin{Bmatrix} J_f & \frac{9}{2} & j_2 \\ \frac{9}{2} & J & 9 \end{Bmatrix}.$$

We have assumed a direct, one-step reaction, with the $1h_{9/2}$ proton merely a spectator in the transfer process. An additional phase factor, $(-1)^{n_1+n_2}$, is required in the above expression to convert conventional shell model radial bound state wave functions (positive near $r=0$) to the DWUCK convention (positive near $r=\infty$). Here, n_1 and n_2 denote the number of nodes (excluding the origin but including $r=\infty$) in the shell model radial wave functions.

The results of the DWBA calculations using the mixed configuration wave functions of Kuo[8] for ^{208}Bi are shown as the solid curves in Figs. 2 and 3. For comparison, calculations carried out assuming pure configurations are also plotted (dashed lines).

A different procedure was used to calculate angular distributions corresponding to several strongly populated levels above 2.4 MeV excitation in ^{208}Bi. As discussed below in detail, these states closely resemble ^{206}Pb core excitations (J_c) weakly coupled to the $(\pi h_{9/2}, \nu g_{9/2})$ target configuration. Thus, we calculated the corresponding ^{210}Bi$^m(p,t)^{208}$Bi transitions in terms of the weak coupling expression,

$$\frac{d\sigma}{d\Omega}(\vec{J}_f = \vec{J}_c + \vec{J}_i) = N_f \frac{2J_f+1}{(2J_c+1)(2J_i+1)} \frac{d\sigma}{d\Omega}(J_c),$$

in which the core-excited wave functions were taken to be those of the ground and first-excited states of ^{206}Pb calculated by Ma and True.[9] Since the above expression relates the observed cross sections in ^{208}Bi to those corresponding to population of the underlying core-excitations, the overall normalization for $(d\sigma/d\Omega)(J_c)$ was chosen in a companion calculation to reproduce the $L=0$ ground state, and $L=2$ first-excited state, yields measured for the ^{208}Pb$(p,t)^{206}$Pb reaction by Erb and Bhatia.[20] The comparison of the DWBA calculations, thus normalized, with the present data determines the individual factors, N_f, and hence the extent to which the ^{206}Pb core strengths are concentrated in the corresponding levels of ^{208}Bi. It should be noted in this context that the DWBA calculations serve merely as a convenient means of accounting for (small) kinematic and Q-value differences between the corresponding ^{208}Pb$(p,t)^{206}$Pb and ^{210}Bi$^m(p,t)^{208}$Bi reactions; by normalizing the DWBA results to the yields measured in the former reaction we have effectively removed the dependence of the factors, N_f, on the detailed assumptions of the DWBA reaction model. The calculated angular distributions, renormalized by the N_f factors listed in Table II, are compared with the relevant data in Figs. 4 and 5.

IV. DISCUSSION

A. Positive-parity $(\pi h_{9/2}, \nu^{-1})$ multiplets

Satisfactory agreement was found between the predicted and measured cross sections corresponding to the population of the positive-parity $(\pi h_{9/2}, \nu^{-1})$ multiplets. A few multiplet members were predicted in the DWBA calculations to be too weakly populated for observation with the thin target used in the present work [notably including the entire $(\pi h_{9/2}, \nu^{-1} h_{9/2})$ multiplet] and indeed these were not seen in the present work. Nine transitions, representing each of the other four $\nu^{-1}(p_{1/2}, f_{5/2}, p_{3/2}, f_{7/2})$ positive-parity multiplets, were sufficiently intense that the corresponding angular distributions could be extracted from the data. These angular distributions are plotted in Fig. 2 with DWBA predictions ($\epsilon=1$) using both pure-configuration wave functions and the mixed configuration results of Kuo.[8] Where the differences between the two calculations are too small to be visible, only the former results are shown.

As the comparison in Fig. 2 illustrates, the Kuo

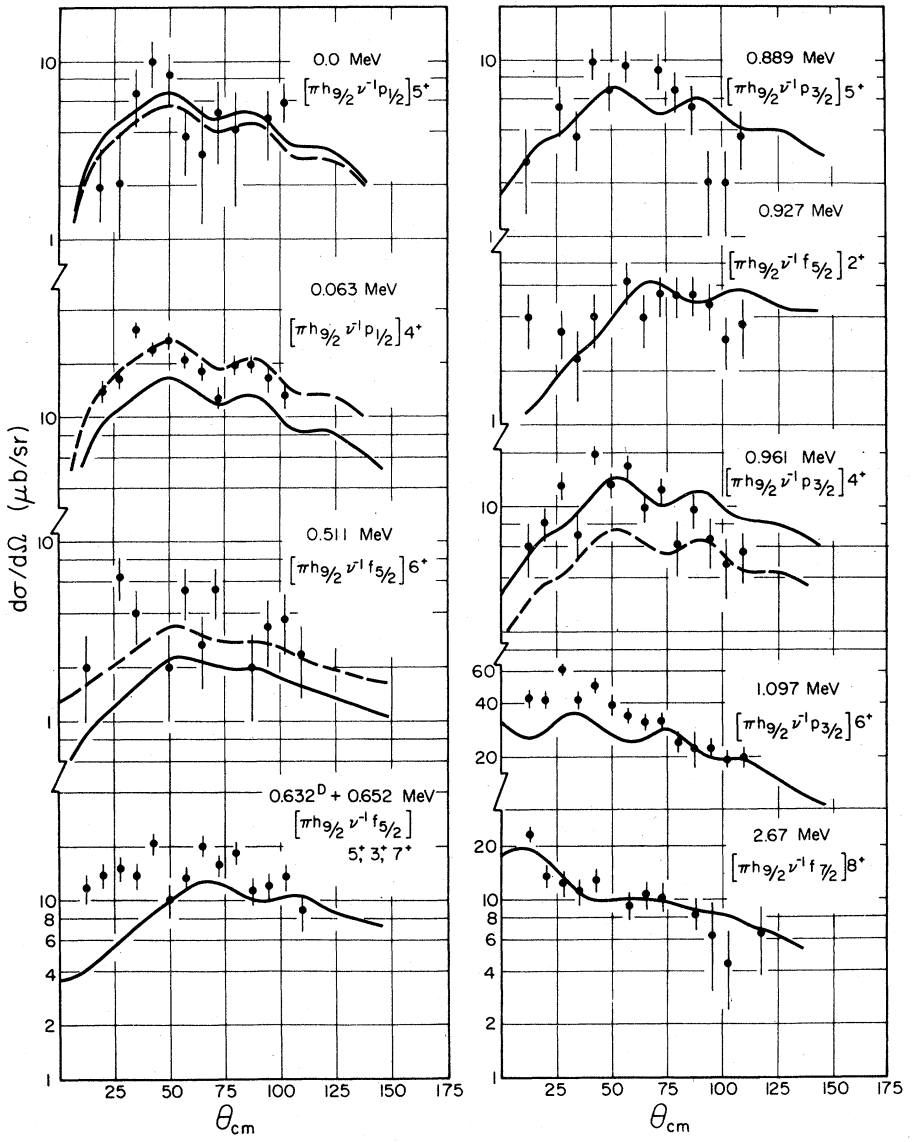

FIG. 2. Angular distributions measured in the ^{210}Bi$^m(p,t)^{208}$Bi reaction for members of the positive parity $(\pi h_{9/2}, \nu^{-1})$ multiplets. DWBA calculations using pure configuration (broken lines) and Kuo, mixed configuration (solid lines), wave functions are also plotted. Aside from an overall normalization, the predicted DWBA cross section magnitudes have not been rescaled to fit the data (i.e., $\epsilon = 1$ for all calculations).

calculations lead to an improved description of the $(\pi h_{9/2}, \nu^{-1}p_{3/2})4^+$ data, but at the expense of somewhat poorer fits to the measured $(\pi h_{9/2}, \nu^{-1}p_{1/2})4^+$ and $(\pi h_{9/2}, \nu^{-1}f_{5/2})6^+$ angular distributions. Even though the Kuo wave functions exhibit a relatively small degree of configuration mixing—amounting in the most extreme case to less than 14% in the squared amplitudes—the small admixtures result in sizable changes in the predicted cross sections. The present data thus provide the opportunity for a detailed and sensitive investigation of the shell model wave functions. A more sophisticated model of the reaction process may be required for this purpose, however, in view of the likely contributions of more complicated nondirect reaction mechanisms,[21,22] and an investigation of this nature falls outside the scope of the present work. For the present, we cite the general agreement between calculated and measured yields for the $(\pi h_{9/2}, \nu^{-1})$ positive-parity multiplets primarily in order to calibrate the gross discrepancies discussed in the next section.

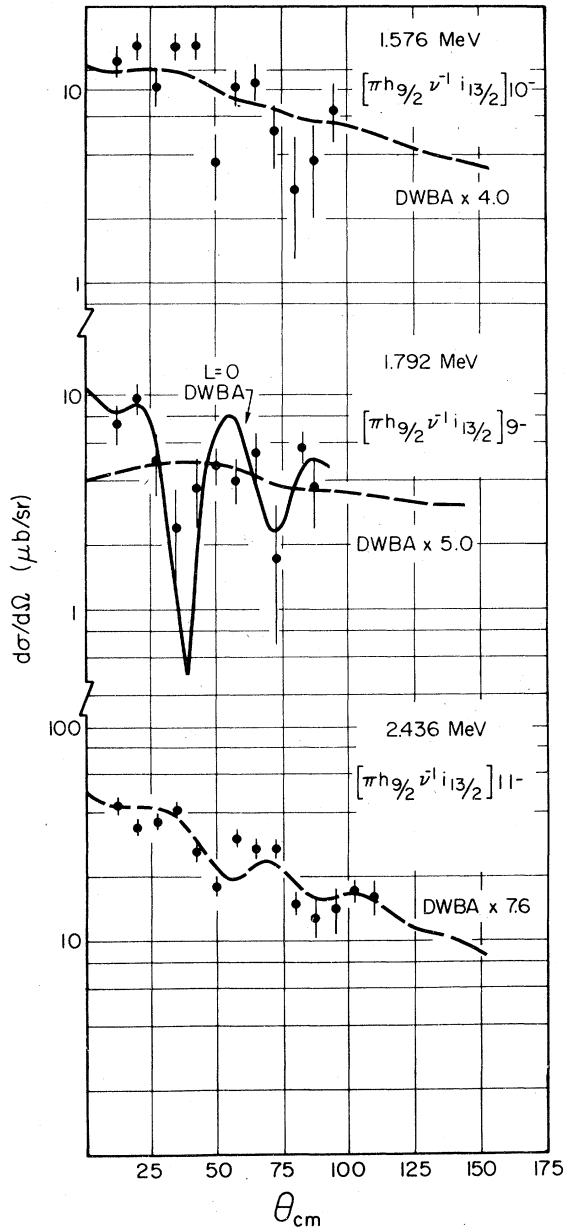

FIG. 3. Angular distributions measured in the $^{210}Bi^m(p,t)^{208}Bi$ reaction for members of the negative parity $(\pi h_{9/2},\ \nu^{-1}i_{13/2})$ multiplet. The one-particle one-hole DWBA calculations illustrated with the broken lines were renormalized by the factors indicated. For comparative purposes, an $L=0$ DWBA calculation is also plotted with the 1.792 MeV data, as discussed in the text.

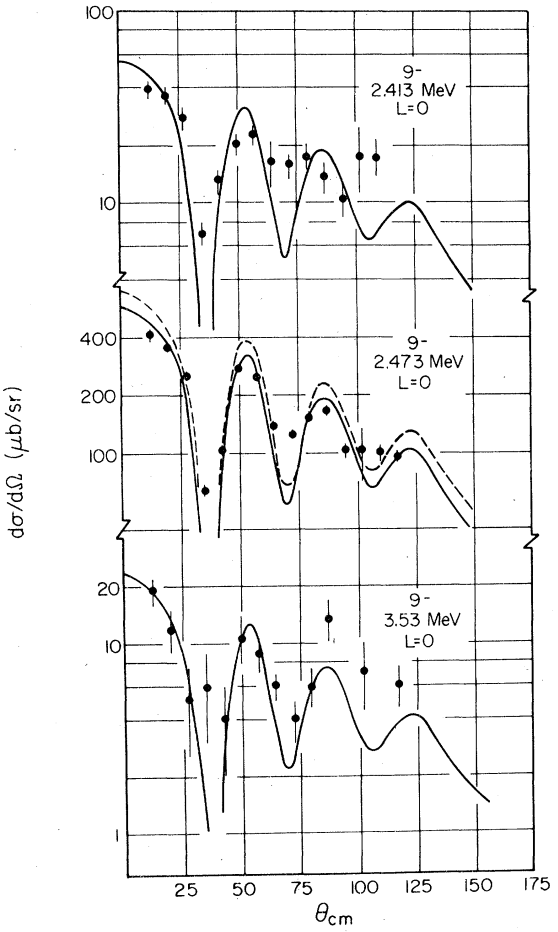

FIG. 4. Angular distributions measured in the $^{210}Bi^m(p,t)^{208}Bi$ reaction corresponding to enhanced $L=0$ transitions. DWBA calculations based on the weak-coupling model are also plotted, using the normalization factors given in Table II. The broken-line curve for the 2.473 MeV data shows the angular distribution corresponding to the unfragmented $^{208}Pb(p,t)^{206}Pb(0_1^+)$ core-excited transition, as discussed in the text.

B. The negative-parity $(\pi h_{9/2}, \nu^{-1} i_{13/2})$ multiplet

In contrast to the situation discussed above for the positive parity multiplets, the data obtained in the present study for the $(\pi h_{9/2}, \nu^{-1} i_{13/2})$ multiplet could not be reproduced by DWBA calculations using the simple shell-model wave functions. Angular distributions were extracted from the data for three members of this multiplet, and these are plotted in Fig. 3. The comparison of the DWBA calculations with the data in Fig. 3 reveals several serious discrepancies.

The predicted cross sections are all much too small in comparison to the measured yields by factors ranging from 4.0 to 7.5. These differences in magnitude are common to the negative-parity multiplet members, and are much larger than any observed for the nine positive-parity levels discussed in the previous section, suggesting a systematic problem not solely a result of deficiencies in the reaction mechanism description.

In addition, an $L=0$ component appears in the

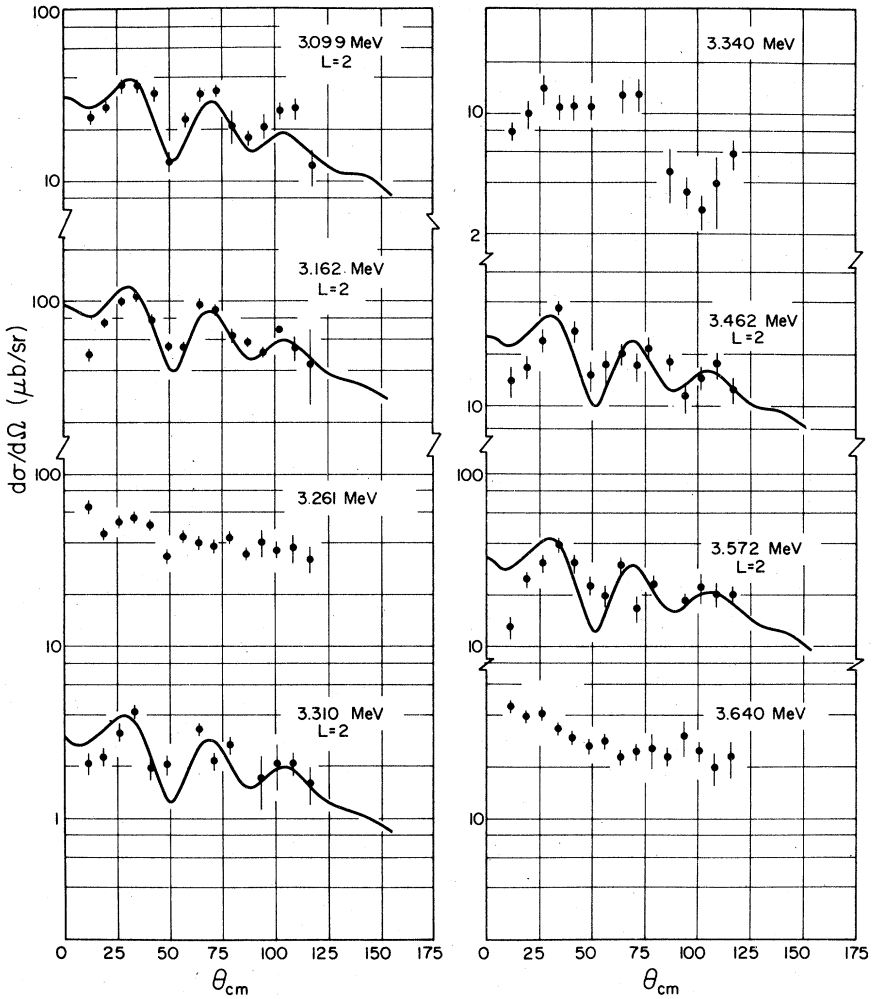

FIG. 5. Angular distributions measured in the ^{210}Bi$^{m}(p,t)^{208}$Bi reaction for strongly populated levels above 3 MeV excitation. DWBA calculations based on the weak-coupling model are also plotted where applicable, using the normalization factors given in Table II.

angular distribution corresponding to the population of the 9$^-$ level. [For purposes of comparison, we have superimposed on these data a renormalized $L=0$ angular distribution calculated using the coherent two-neutron-hole ^{206}Pb(0_1^+) wave function of Ma and True. The shape of this curve is a completely unambiguous indication of the $L=0$ angular momentum transfer, and is essentially independent of the details of the transfer form factor.] The direct $L=0$ transfer is *strictly forbidden* for the $(\pi h_{9/2}, \nu^{-1} i_{13/2})$ residual state configuration, because of the $(\pi h_{9/2}, \nu g_{9/2})$ target structure. This observation, and the enhanced cross sections observed for all three transitions plotted in Fig. 3, suggest the presence of additional, sizable wave function components in these negative parity states. There are no other low-lying negative-parity one-particle one-hole multiplets containing an $h_{9/2}$ proton with which these levels can mix, so we conclude that two-particle two-hole (i.e., core-excited) configurations may be present. Additional evidence for this conclusion may be adduced from our observation, discussed below, of strongly populated core-excited states in this general excitation energy region. The possible importance of two-particle two-hole admixtures was suggested previously on theoretical grounds by Ma and True,[9] but calculations incorporating these additional configurations have not yet been reported.

C. Two-particle two-hole, core-excited states

The levels at 2.473 and between 3.1 and 3.6 MeV excitation dominate the spectra measured in the ^{210}Bi$^{m}(p,t)^{208}$Bi reaction (Fig. 1). With a few exceptions, the corresponding angular distributions

shown in Figs. 4 and 5 are characteristic of either $L=0$ or $L=2$ transfer, as the comparison with the DWBA curves in the figures illustrates. This establishes the negative parity of most of these states, and also shows that they can not be identified with the members of the $(\pi h_{9/2}, \nu^{-1}h_{9/2})$ multiplet which occur in this excitation energy region. The measured cross sections are, for the most part, significantly larger than those associated with transitions leading to pure one-particle one-hole configurations and can only be reproduced by DWBA calculations when contributions from several configurations are allowed to interfere constructively.

1. $L=0$ transitions

The 2.473 MeV excitation energy of the 9^- state populated in the very intense $L=0$ $^{210}\mathrm{Bi}^m(p,t)^{208}\mathrm{Bi}$ transition corresponds very closely to the energy at which the two-particle two-hole $[(\pi h_{9/2}, \nu g_{9/2})_{9^-} \otimes {}^{206}\mathrm{Pb}(0_1^+)]$ excitation would occur in ^{208}Bi. In the absence of residual interactions among the three components of the configuration, the excitation would appear at

$$\begin{aligned} E_x &= E(\pi h_{9/2}) + E(\nu g_{9/2}) + E(\nu^{-2} J=0) - E(^{208}\mathrm{Bi\ g.s.}) \\ &= B(^{209}\mathrm{Bi}) + B(^{209}\mathrm{Pb}) + B(^{206}\mathrm{Pb}) - B(^{208}\mathrm{Bi}) \\ &= 2.710 \text{ MeV}. \end{aligned}$$

(For these estimates we have used binding energies relative to ^{208}Pb deduced from the mass-excess compilation of Wapstra and Bos.[23]) To this value the following empirical estimates for the residual interaction energies should be added:

$$\begin{aligned} \Delta E(\pi h_{9/2}, \nu^{-2} J=0) &= B(^{207}\mathrm{Bi}) - B(^{209}\mathrm{Bi}) - B(^{206}\mathrm{Pb}) \\ &= +0.246 \text{ MeV}, \\ \Delta E(\nu g_{9/2}, \nu^{-2} J=0) &= B(^{207}\mathrm{Pb} g_{9/2}, E_x = 2.728 \text{ MeV}) \\ &\quad - B(^{209}\mathrm{Pb}) - B(^{206}\mathrm{Pb}) \\ &= -0.075 \text{ MeV}, \\ \Delta E(\pi h_{9/2}, \nu g_{9/2})_{9^-} &= B(^{210}\mathrm{Bi}\, 9^-, E_x = 0.271 \text{ MeV}) \\ &\quad - B(^{209}\mathrm{Pb}) - B(^{209}\mathrm{Bi}) \\ &= -0.397 \text{ MeV}. \end{aligned}$$

Thus, the $[(\pi h_{9/2}, \nu g_{9/2})_{9^-} \otimes {}^{206}\mathrm{Pb}(0_1^+)]_{9^-}$ excitation is estimated at 2.484 MeV excitation in ^{208}Bi, in close proximity to the observed 2.473 MeV 9^- level.

Unless the above agreement between calculated and observed 9^- excitation energies is merely fortuitous, the small magnitude of the discrepancy (11 keV) indicates that the weak coupling model can be used to calculate the corresponding $^{210}\mathrm{Bi}^m(p,t)^{208}\mathrm{Bi}$ cross section. The dashed-line curve superimposed on the 2.473 MeV data in Fig. 4 was calculated on this assumption, following the procedure discussed in Sec. III, and is based on DWBA calculations which reproduce the observed $^{208}\mathrm{Pb}(p,t)^{206}\mathrm{Pb}$ ground state yields. The result closely approximates the measured yields for the 2.473 MeV 9^- level and thus provides very strong evidence for $[(\pi h_{9/2}, \nu g_{9/2})9^- \otimes {}^{206}\mathrm{Pb}(0^+)]$ structure. Since quantitative agreement between the data and the calculation may be achieved with a renormalization factor for the latter of 0.82 (Table II and solid curve in Fig. 4), we conclude that nearly all the $^{206}\mathrm{Pb}(0_1^+)$ core strength resides in the 2.473 MeV level. A final indication of $^{206}\mathrm{Pb}(0_1^+)$ parentage appears if we identify the 2.473 MeV level with the state observed at 2.477 MeV in the $^{206}\mathrm{Pb}(\alpha,d)^{208}\mathrm{Bi}$ measurements of Daehnick *et al.*[24]

Two additional $L=0$ transitions, resulting from the population of levels at 2.413 and 3.530 MeV excitation in ^{208}Bi, were observed in the present work, and the corresponding angular distributions are plotted in Fig. 4. The solid curves were calculated in the weak coupling approximation discussed above, and were normalized to best fit the data using the factors listed in Table II. The characteristic $L=0$ angular distributions show that these are $J^\pi = 9^-$ states, and thus the 2.413 MeV level is distinct from the state observed near this excitation energy via $L=3$ transfer in the $^{209}\mathrm{Bi}(d,t)^{208}\mathrm{Bi}$ and $^{209}\mathrm{Bi}(p,d)^{208}\mathrm{Bi}$ reactions. [The latter state is the 6^+ member of the $(\pi h_{9/2}, \nu^{-1} f_{7/2})$ multiplet.[25]] The nature of the 2.413 and 3.530 MeV excitations is unknown, but the former, at least, probably contains a two-particle two-hole wave function component in view of its 8% share of the $^{206}\mathrm{Pb}(0_1^+)$ core-excitation strength.

Given the close proximity of the 2.413 and 2.473 MeV 9^- levels to each other and to the predicted position of the $[(\pi h_{9/2}, \nu g_{9/2})_{9^-} \otimes {}^{206}\mathrm{Pb}(0_1^+)]$ core-excited configuration, it is natural to identify both levels as fragments of the underlying core excitation. Together, they exhaust 90% of the associated $^{210}\mathrm{Bi}^m(p,t)^{208}\mathrm{Bi}$ transition strength (Table II). This survival of the intrinsic $^{206}\mathrm{Pb}(0_1^+)$ structure in the presence of two additional valence nucleons underscores its remarkable stability, and permits the very simple weak-coupling interpretation of these complicated two-particle two-hole excitations in ^{208}Bi.

2. $L=2$ transitions

The successful weak-coupling description of the $L=0$ cross sections implies that a quintuplet of relatively intense $L=2$ transitions, corresponding to the coupling of the 2_1^+ ^{206}Pb core excitation ($E_x = 0.803$ MeV) with the $(\pi h_{9/2}, \nu g_{9/2})9^-$ target con-

figuration, should be observed near 3.3 MeV in the ^{210}Bi$^m(p,t)^{208}$Bi reaction. Several candidates appear between 3.1 and 3.7 MeV in the spectrum of Fig. 1, and of the seven corresponding angular distributions plotted in Fig. 5, five were found to be characteristic of $L=2$ transfer. The curves in the figure were calculated using the weak-coupling procedure discussed in Sec. III, and were renormalized by the factors in Table II to fit the data. A level-by-level comparison of the model predictions with the data is impossible in the absence of spin assignments, but it is significant that the combined $L=2$ strength measured in the ^{210}Bi$^m(p,t)^{208}$Bi reaction represents some 75% of that anticipated from the weak-coupling model.

The splitting apart of the multiplet candidates is qualitatively similar to that observed in data from the analogous ^{209}Bi$(p,t)^{207}$Bi reaction.[20] In the latter case, the members of the $[\pi h_{9/2} \otimes {}^{206}\mathrm{Pb}(2_1^+)]$ quintuplet also were found to be spread over an excitation energy interval of 0.5 MeV. In addition, 80% of the ^{208}Pb$(p,t)^{206}$Pb(2_1^+) core excitation strength was recovered in the ^{207}Bi quintuplet, in close similarity with the results of the present work. The ^{209}Bi$(p,t)^{207}$Bi $L=2$ cross sections—although suitably enhanced—were not distributed among the quintuplet according to the $(2J_f+1)$ rule implied by the simple weak-coupling model, and for this reason we have not attempted in the present study to make spin assignments on the basis of cross section magnitudes. A better theoretical treatment is needed to reproduce these yields in detail, but the parallels among the "enhanced" $L=2$ transitions observed in the ^{208}Pb$(p,t)^{206}$Pb, ^{209}Bi$(p,t)^{207}$Bi, and ^{210}Bi$^m(p,t)^{208}$Bi reactions clearly demonstrate the survival of the ^{206}Pb(2_1^+) core strength in the two-particle two-hole spectrum of ^{208}Bi.

V. CONCLUSION

The ^{210}Bi$^m(p,t)^{208}$Bi reaction was found to be a sensitive probe of two-particle two-hole structure in ^{208}Bi. One such state, based on the weak-coupling $[(\pi h_{9/2}, \nu g_{9/2})_{9^-} \otimes {}^{206}\mathrm{Pb}(0_1^+)]$ configuration, was identified at 2.473 MeV in ^{208}Bi. The observed excitation energy of this level, and the corresponding differential cross sections, were found to imply that the ^{206}Pb(0_1^+) core excitation survives essentially intact in ^{208}Bi despite the presence of two additional nucleons. In addition, several levels were observed between 3.1 and 3.7 MeV excitation which were found to have a sizable parentage in the ^{206}Pb(2_1^+) core excitation.

The measured cross sections corresponding to the population of positive parity one-particle one-hole levels in ^{208}Bi were well described by DWBA calculations using the shell model wave functions of Kuo. The present data, together with a more detailed treatment of the reaction process incorporating nondirect transfer mechanisms, should provide a sensitive test of these wave functions. In addition, the experiment provides the first indications of two-particle two-hole admixtures in the wave functions of several members of the $(\pi h_{9/2}, \nu^{-1} i_{13/2})$ multiplet, demonstrating the need for shell model calculations using an enlarged model space.

ACKNOWLEDGMENTS

The authors gratefully acknowledge the contributions of Mr. David Mankoff and Dr. George Holland to this work. This research was supported under U.S.D.O.E. Contract No. EY-76-C-02-3074, and NSF Grant No. PHY77-12876.

---

*Present address: Malden Public Schools, Malden, Mass. 02148.

[1]J. R. Erskine, Phys. Rev. 135, B110 (1964).
[2]W. P. Alford, J. P. Schiffer, and J. J. Schwartz, Phys. Rev. Lett. 21, 156 (1968); Phys. Rev. C 3, 860 (1971).
[3]D. Proetel, M. Dost, E. Grosse, H. J. Körner, and P. Von Brentano, Nucl. Phys. A161, 565 (1971).
[4]G. M. Crawley, E. Kashy, W. Lanford, and H. G. Blosser, Phys. Rev. C 8, 2477 (1973).
[5]C. Ellegaard, P. D. Barnes, and T. R. Canada, Phys. Rev. C 7, 742 (1973).
[6]J. P. Schiffer and W. W. True, Rev. Mod. Phys. 48, 191 (1976), and references therein.
[7]Y. E. Kim and J. O. Rasmussen, Phys. Rev., 135, B44 (1964).
[8]T. T. S. Kuo, Nucl. Phys. A122, 325 (1968).
[9]C. W. Ma and W. W. True, Phys. Rev. C 8, 2313 (1973), and unpublished tables.
[10]D. G. Kovar, C. K. Bockelman, W. D. Callender, L. J. McVay, C. F. Maguire, and W. D. Metz, Wright Nuclear Structure Laboratory Internal Report No. 49, 1970 (unpublished).
[11]R. Leonard, R. L. Ponting, and R. K. Sheline, Nucl. Instrum. Methods 100, 459 (1972).
[12]P. D. Kunz, University of Colorado (unpublished).
[13]F. G. Perey, Phys. Rev. 131, 745 (1963).
[14]E. R. Flynn, G. Igo, P. D. Barnes, D. Kovar, D. Bes, and R. Broglia, Phys. Rev. C 3, 2371 (1971).
[15]H. W. Baer, J. J. Kraushaar, C. E. Moss, N. S. P. King, R. E. L. Green, P. D. Kunz, and E. Rost, Ann. Phys. (N.Y.) 76, 437 (1973).
[16]J. B. Ball, R. L. Auble, and P. G. Roos, Phys. Rev.

C 4, 196 (1971).
[17]S. Yoshida, Nucl. Phys. 33, 685 (1962).
[18]J. J. Kolata and W. W. Daehnick, Phys. Rev. C 5, 568 (1972).
[19]C. K. Cline, W. P. Alford, H. E. Gove, and R. Tickle, Nucl. Phys. A186, 273 (1972).
[20]Karl A. Erb and T. S. Bhatia, Phys. Rev. C 7, 2500 (1973).
[21]R. J. Ascuitto and N. K. Glendenning, Phys. Rev. C 2, 1260 (1970); L. A. Charlton, *ibid.* 14, 506 (1976); M. Strayer and M. Werby, J. Phys. G 3, L179 (1977).
[22]N. B. de Takacsy, Nucl. Phys. A231, 243 (1974).
[23]A. H. Wapstra and K. Bos, At. Data Nucl. Data Tables 19, 175 (1977); 20, 1 (1977); Errata: At. Data Nucl. Data Tables 20, 126 (1977).
[24]W. W. Daehnick, M. J. Spisak, R. M. DelVecchio, and W. Oelert, Phys. Rev. C 15, 554 (1977).
[25]M. B. Lewis, Nucl. Data B5 (No. 5), 243 (1971).